

# THE EXTRAPOLATION OF HIGH ALTITUDE SOLAR CELL I(V) CHARACTERISTICS TO AM0

David B. Snyder<sup>†</sup>, David A. Scheiman<sup>‡</sup>, Phillip P. Jenkins<sup>¶</sup>,  
William Reike<sup>†</sup>, Kurt Blankenship<sup>†</sup>, James Demers<sup>†</sup>

<sup>†</sup>NASA Glenn Research Center, Cleveland Ohio

<sup>‡</sup>Essential Research, Cleveland, Ohio

<sup>¶</sup>OAI, Cleveland, Ohio

## Abstract

The high altitude aircraft method has been used at NASA GRC since the early 1960's to calibrate solar cell short circuit current,  $I_{SC}$ , to Air Mass Zero (AM0). This method extrapolates  $I_{SC}$  to AM0 via the Langley plot method, a logarithmic extrapolation to 0 air mass, and includes corrections for the varying Earth-Sun distance to 1.0 AU and compensating for the non-uniform ozone distribution in the atmosphere. However, other characteristics of the solar cell I(V) curve do not extrapolate in the same way. Another approach is needed to extrapolate  $V_{OC}$  and the maximum power point ( $P_{MAX}$ ) to AM0 illumination. As part of the high altitude aircraft method,  $V_{OC}$  and  $P_{MAX}$  can be obtained as  $I_{SC}$  changes during the flight. These values can then be extrapolated, sometimes interpolated, to the  $I_{SC}(AM0)$  value. This approach should be valid as long as the shape of the solar spectra in the stratosphere does not change too much from AM0. As a feasibility check, the results are compared to AM0 I(V) curves obtained using the NASA GRC X25 based multi-source simulator. This paper investigates the approach on both multi-junction solar cells and sub-cells.

## 1 Introduction

### 1.1 Background

The present goal of terrestrial flight calibration is to provide the calibrated short circuit current,  $I_{SC}$ , for primary standard solar cells to ground-based laboratories so the intensity of solar simulators can be adjusted to on-orbit conditions. This level of illumination is called Air Mass Zero, AM0, since there is no atmospheric adsorption of the solar spectrum. In addition these measurements are standardized to an Earth-Sun distance,  $R_{SE}$ , of 1.0 AU. This system works well for single junction solar cells. However, for multi-junction solar cell measurements, the accuracy of the laboratory spectrum becomes more important. An empirical comparison with the measurements using the solar spectrum will increase the confidence in laboratory results.

Three facilities exist to calibrate primary standards to AM0 (1-3). JPL and CNES use a high altitude balloon fly solar cells above 99.5% of the atmosphere. NASA GRC uses a Lear 25 to take data above 90% to 80% of the atmosphere. The measurements are then extrapolated to zero pressure. Round-robin comparisons of single junction solar cells shows the three methods agree to about 1% (1). A recent round-robin measurement of triple-junction solar cells shows the three facilities also agree to within 1% (4).

The high altitude flight calibration method for characterizing solar cell short circuit currents,  $I_{SC}$ , has been used at NASA Glenn Research Center since the 1963 (5). The NASA GRC flight calibration facility flies in the stratosphere to avoid most of the water vapor, and aerosols in the troposphere (6). It flies in the winter when the tropopause is low and  $R_{SE}$  is less than 1 AU. The cells are flown in a manned aircraft, so the system is low risk, i.e the probability of the cells returning is very high. This method consists of taking  $I_{SC}$  measurements of solar cells illuminated by the sun as the aircraft descends from near 50 kft to the tropopause, often near 35 kft in the winter. This data can be adjusted for atmospheric ozone adsorption and the Earth-Sun distance, then extrapolated to zero pressure using the Langley Plot method. The measurement temperature is controlled at 25 C, or 28 C. A principal advantage of this method, is the ability to re-fly cells on short notice, even the next day. A typical winter flying season consists of 20 to 30 flights. Corrections are included for  $R_{SE} = 1$  AU, and ozone adsorption (7,8) of

the solar spectra, The measurements are taken as the plane descends from nearly 50 kft to 35 kft, and are extrapolated via a semi-log fit to zero pressure. The optical air mass typically ranges from 0.2 to 0.4. The results of this system are consistent with the balloon methods (1,4). In addition to  $I_{SC}$ , the NASA GRC data acquisition system has the capability of measuring open circuit voltage ( $V_{OC}$ ) and current-voltage curves ( $I(V)$ ). For the past three years, most flights have included  $I(V)$  measurements of the cells flown.

All three methods can be used to obtain  $I(V)$  curves of solar cells in low air mass conditions, but the resulting flight data may generally not be representative of AM0. All methods require some correction to standardized AM0 conditions. This paper presents a method to use that data to characterize  $I(V)$  parameters at AM0 illumination from flight data.

Several corrections are made to  $I_{SC}$  calibration measurements, whether made by balloon or high altitude aircraft, to convert them to AM0 illumination at an Earth-Sun distance ( $R_{SE}$ ) of 1 AU. These corrections use the proportionality of  $I_{SC}$  to illumination for scaling the results. Multiplication by  $R_{SE}^2$ , converts the result to  $R_{SE} = 1$  AU. Additional corrections to account for nonzero atmospheric pressure, temperature corrections, and nonuniform ozone distribution may also be included (2).

How to include these corrections into flight  $I(V)$  curve measurements is less clear since parameters such as  $V_{OC}$  and Maximum Power ( $P_{MAX}$ ) may not be proportional to illumination. However, understanding how to make these extrapolations is important for comparing  $I(V)$  curve parameters between flight and laboratory measurements, especially for multi-junction solar cells, which are more sensitive to the source spectrum than single junction cells.

## 1.2 Objectives

The objective of this work is to explore a method of extrapolating  $I(V)$  curve characteristics, such as  $P_{MAX}$  and  $V_{OC}$ , to AM0 and  $R_{SE} = 1$  AU. This method is especially suited for use with the high altitude aircraft method of solar cell calibration. This paper investigates the first two steps in verifying this method. The feasibility of the method will be investigated, and results will be compared with measurements from a laboratory multi-source solar simulator. The third step of comparison with high altitude balloon measurements or spacecraft measurements is left for future work.

## 1.3 Model

### 1.3.1 Single Junction Solar Cell Response

Some observations on the performance of a single junction solar cell may be drawn from a simple qualitative formulation. The conclusions drawn from this model, while not rigorous, can be used to propose empirical extrapolation methods. In addition, the model can be used to suggest validity criteria to check against observations.

Following Woodyard (2), the current,  $I(V)$ , of a single junction solar cell is determined by its spectral response,  $R(\lambda, V)$  and the source spectral irradiance,  $S(\lambda)$ .

$$I(V) = \int_{\lambda_1}^{\lambda_2} S(\lambda) R(\lambda, V) d\lambda \quad (1)$$

For an ideal solar cell, the response function,  $R(\lambda, V)$ , is high, nearly 1, and therefore relatively independent of wavelength in the range  $\lambda_1$  to  $\lambda_2$ . Outside that range (for example, above the band gap wavelength) the cell is not responsive,  $R(\lambda) = 0$ . In this case,

$$I(V) = R(V) \int_{\lambda_1}^{\lambda_2} S(\lambda) d\lambda \quad (2)$$

and the current depends only on, and is linear with, the total irradiance in the interval  $\lambda_1$  to  $\lambda_2$ .  $I(V)$  measurements will be reliable, as long as the total irradiance in the interval is correct. This is especially true for high efficiency cells, where the quantum efficiency is near unity over the active wavelengths.

In addition, if  $R(\lambda, V)$  can be separated into two independent functions,  $Q(\lambda) \cdot R'(V)$ , where  $Q$  is related to the Quantum efficiency, and  $R'$  contains the voltage dependence, then,

$$I(V) = R'(V) \int_{\lambda_1}^{\lambda_2} S(\lambda) Q(\lambda) d\lambda \quad (3)$$

While not linear with the total irradiance,  $R'(V)$  contains the voltage dependence and a value for  $I_{SC}$  specifies the  $I(V)$  curve. This suggests that extrapolation of  $I(V)$  curve parameters, especially for short ranges of  $I_{SC}$  is reasonable. Since the shape of  $I(V)$  is given by  $R'(V)$ , changes in  $V_{OC}$  and  $V_{MAX}$  with irradiance are not expected, or at most will be small, and can be used to verify applicability of the extrapolation.

### 1.3.2 Multi-junction Solar Cell Response

Multi-junction solar cells are more sensitive to details of the spectrum. Each junction of a triple-junction cell operates along its own  $I(V)$  curve. However, the current through each junction is the same.

$$\begin{aligned} I(V) &= \int_{\lambda_1}^{\lambda_2} S(\lambda) R_1(\lambda, V_1) d\lambda \\ &= \int_{\lambda_3}^{\lambda_4} S(\lambda) R_2(\lambda, V_2) d\lambda \\ &= \int_{\lambda_5}^{\lambda_6} S(\lambda) R_3(\lambda, V_3) d\lambda \end{aligned} \quad (4)$$

where  $V = V_1 + V_2 + V_3$ . As a result, the cell that supports the least current dominates the  $I(V)$  behavior of the multi-junction cell.  $V_{OC}(I=0)$  is determined by the sum of the junction  $V_{OC}$ 's, and is therefore expected to have only a weak dependence on irradiance like the single junction cell.  $I_{SC}$ , however, is dominated by the current limiting junction. That junction will be reverse biased somewhat because the other junctions are not operating at  $I_{SC}$  for those junctions. Regardless, unless operating near diode breakdown conditions,  $I_{SC}$  for the triple junction cell will be near that of the current limiting junction, and will behave similarly with varying illumination. The maximum power point,  $P_{MAX}$ , will be dominated by the junction that supports the least current. The other junctions will operate at currents somewhat less than  $I_{MAX}$  for those junctions, where  $I(V)$  is changing rapidly with voltage nearer  $V_{OC}$  of the junction.  $V_i$  in those junctions does not change significantly as the current through the junction changes.

As with the single junction cell, as long as each portion of the spectrum is close enough for each junction, the measurement of  $P_{MAX}$  should be accurate.

## 2 Procedure

### 2.1 Method

The extrapolation to AM0 method is quite simple. For single junction cells, as long as the wavelength dependence is weak, extrapolation by  $I_{SC}$ , as a defining parameter of the  $I(V)$  curve to  $I_{SC}(AM0)$  is reasonable. Checks on the validity of the extrapolation are a linear dependence of  $I_{MAX}$  on  $I_{SC}$ , and weak dependence of  $V_{OC}$  and  $V_{MAX}$  on  $I_{SC}$ . Initially, this analysis was based on logarithmic fits of the data. However, this confirmed the linear dependence of  $I_{MAX}$  and weak dependence of  $V_{OC}$  and  $V_{MAX}$  on  $I_{SC}$ . In this paper, the linear extrapolations are presented.

#### 2.1.1 Quadratic Fit Equation

Since this work will be looking at effects due to small changes in light intensity, it is important to have precise and accurate values for  $P_{MAX}$ . While current measurements are very precise, the number of points in the  $I(V)$  curve, determined by the number of applied voltages, is limited to 20 to 40 points and uncertainties in  $V_{MAX}$  may be greater than 2%. This also limits the accuracy of  $I_{MAX}$ , depending on how rapidly it changes over the interval. However, since the  $I(V)$  curve varies smoothly in this region, it is easy to interpolate using a quadratic fit between the three points nearest  $P_{MAX}$ . From the coefficients of the fit, the voltage,  $V_{MAX}$ , where  $dP_{MAX}/dV = 0$  can be found.  $I_{MAX}$  and  $P_{MAX}$  follow readily from  $V_{MAX}$ .

The quadratic equation through three arbitrary points,  $(x_1, y_1)$ ,  $(x_2, y_2)$ ,  $(x_3, y_3)$ , has the form<sup>9</sup>:

$$y(x) = \frac{(x-x_2)(x-x_3)y_1}{(x_1-x_2)(x_1-x_3)} + \frac{(x-x_1)(x-x_3)y_2}{(x_2-x_1)(x_2-x_3)} + \frac{(x-x_1)(x-x_2)y_3}{(x_3-x_1)(x_3-x_2)} \quad (5)$$

where  $x$  is the electrical power ( $I^*V$ ) and  $y$  may be either  $I$  or  $V$ . The maximum power point is found from the derivative  $dy/dx$ :

$$dy/dx = -\frac{((x-x_2)x_3 + x_2(x-x_3))y_1}{(x_1-x_2)(x_1-x_3)} - \frac{((x-x_1)x_3 + x_1(x-x_3))y_2}{(x_2-x_1)(x_2-x_3)} - \frac{((x-x_1)x_2 + x_1(x-x_2))y_3}{(x_3-x_1)(x_3-x_2)} \quad (6)$$

where  $dy/dx = 0$ .

## 2.2 Assumptions

The principle assumption contained in this method is that the shape of the spectrum does not vary enough to be significant throughout the measurement region, and it is close enough to the AM0 shape. This is so the response of the sub-cells does not change much. This raises an important concern in its application to the high altitude aircraft method especially with regard to the ozone layer above the aircraft. This is an issue to be aware of, but in this work it did not appear to be important in the comparison with the laboratory AM0 spectrum. The principal concern is that a cell that is limited by one junction in an AM0 spectrum is, due to spectral changes, limited by a different junction in the flight measurements. This has not yet been observed.

This method assumes  $I_{SC}$  is well known. Uncertainties in  $I_{SC}$  can be used to estimate uncertainties in  $I_{MAX}$  and  $V_{MAX}$ .

**Table 1. Solar Cells used for Extrapolation Feasibility investigation.**

Name	Type	Average (mA)	St Dev (mA)
SL7733X8	GaInP (Top)	69.91	0.25
SL6726X9	GaAs (Mid)	70.27	0.17
SL9640A5	Ge (Bottom)	131.89	0.36
SL6265X3	TJ	68.52	0.29

## 2.3 Test Cells

The solar cells used in this investigation are a set of 2x2 cm triple junction solar cells procured from SpectroLab. The set includes a triple junction cell and three individual sub-cells. The following table shows the  $I_{SC}$  values obtained from 6 flights with the standard deviations of the six measurements. Using these four solar cells, while not a complete survey of cell technologies, provides a look at solar cells with a variety of work functions.

## 2.4 Procedure

Each of the four solar cells were flown six times on the Lear 25 during the 2004-05 flight season. Flight conditions are given in Table 2. A description of flight procedure is given in reference 6. Normally, the flight data set includes atmospheric pressure, test plate temperature,  $I_{SC}$ , and  $V_{OC}$ . In addition, during the flights an  $I(V)$  curve was taken every third data cycle. Six to seven sets of  $I(V)$  curves were taken for each solar cell on each flight.

**Table 2. Flight Conditions for Triple Junction and sub-cells.**

	Flt#08	Flt#09	Flt#16	Flt#17	Flt#18	Flt#19
Date	02/10/05	02/11/05	03/04/05	03/08/05	03/15/05	03/16/05
Res (AU)	0.9870	0.9871	0.9918	0.9928	0.9946	0.9949
Sun Alt (deg)	30.85	31.18	38.80	40.35	43.11	43.50
Tropopause (mb)	310	330	310	450	390	450
Ozone (DU)	361	402	409	426	348	340

## 3 Results

This section summarizes the flight data. Because this work is intended to investigate the feasibility of the technique, the data from the six flights is analyzed together rather than separately. To the extent that the flight-to-flight data is indistinguishable indicates reproducibility.

**Figure 1.** Flight data of  $V_{OC}$  of a triple junction solar cell.

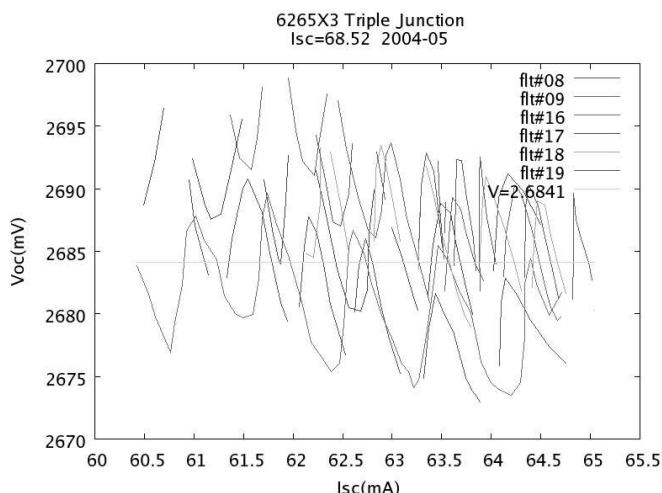


Table 3 shows these values with the standard deviation for  $V_{OC}$  taken from the I(V) curves. In addition the slopes of the linear fits of  $V_{OC}(I_{SC})$  are shown with the slope standard deviation. The slopes are small, and the standard deviations are a significant fraction of the slope. This observation is consistent with the model described above, that the dependence of  $V_{OC}$  on  $I_{SC}$  is weak. Because of the small drift in temperature as the plane descends, the use of the average  $V_{OC}$  seems the most prudent approach.

### 3.1 $V_{OC}$

$V_{OC}$  depends much more on temperature than on illumination and  $I_{SC}$ . The plots of  $V_{OC}$  vs  $I_{SC}$  shown in figure 1 are relatively flat with oscillations due to temperature fluctuations. A few flights show a slightly decreasing  $V_{OC}$  with increasing  $I_{SC}$ . This is counter intuitive since if it had any dependence,  $V_{OC}$  would be expected to increase with illumination and  $I_{SC}$ . It is most likely that this is due increased cooling of the cells as the pressure in the cold stratosphere increases. On this basis, the average  $V_{OC}$  is used to characterize the cells.

The data plotted in Figure 1 is from the usual flight data stream which includes temperature,  $I_{SC}$  and  $V_{OC}$ . It is taken at approximately 10 second intervals.

For this work the  $V_{OC}$  measurements are averaged since only a small  $I_{SC}$  dependence is observed.

**Table 3.** Average  $V_{OC}$  and slope of linear fit.

Type	$\langle V_{OC} \rangle$	$\sigma$	Slope ( $dV_{OC}/dI_{SC}$ )	$\sigma_{slope}$
GaInP (Top)	-1.422	0.003	0.0012	0.0004
GaAs (Mid)	-0.993	0.002	0.0012	0.0006
Ge (Bottom)	-0.257	0.002	-0.0002	0.0004

### 3.2 $I_{MAX}$

The maximum power point,  $P_{MAX}$ , is described by its two components, the current,  $I_{MAX}$ , and the voltage,  $V_{MAX}$ , at that point. First,  $I_{MAX}$  is examined. Figure 2 shows both  $I_{MAX}$  and  $V_{MAX}$  plotted against  $I_{SC}$ . It is apparent that the  $I_{MAX}$  data is nearly linear as suggested earlier.

**Figure 2.** Maximum Power Point,  $V_{MAX}$  and  $I_{MAX}$ , for a triple junction cell plotted against  $I_{SC}$ .

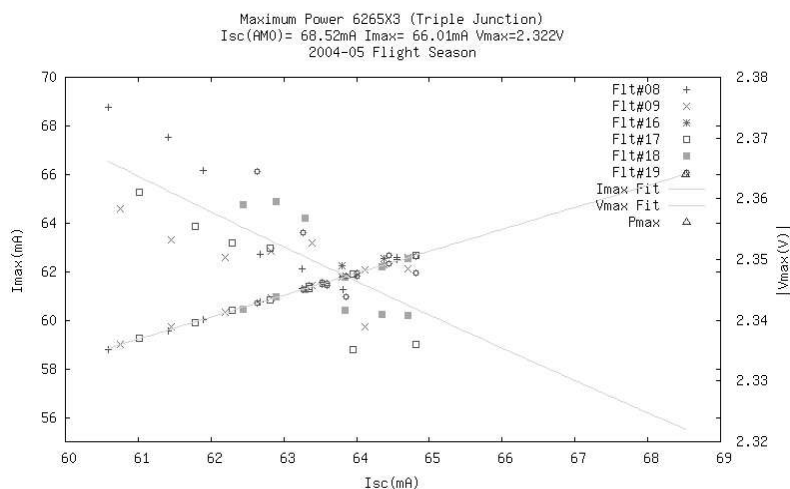


Table 4 shows the linear fit coefficients for  $I_{MAX}(I_{SC})$  of the four cells to the form  $I_{MAX}(I_{SC}) = \langle I_{MAX} \rangle + m(I_{SC} - \langle I_{SC} \rangle)$ . The linear assumption extrapolates back to near zero as indicated by the relatively small y-intercepts suggesting  $I_{MAX}$  is proportional to  $I_{SC}$ .

### 3.3 $V_{MAX}$

$V_{MAX}$  is expected to be independent of, or weakly dependent on,  $I_{SC}$ . Table 5 compares the average  $V_{MAX}$  value with the standard deviation,  $\sigma_{V_{MAX}}$ , and the slope of a linear fit with  $\sigma_{Slope}$ . Since dependence of  $V_{OC}$  is thought to be principally due to temperature effects, that is also of concern here. Figure 2. above shows the dependence of  $V_{MAX}$  on  $I_{SC}$  and a weak dependence is observed.

Comparing with  $\sigma_{V_{OC}}$  in table 3, shows that the standard deviations are similar. If an additional dependence were important over the range of values a higher standard deviation would be expected. However, except for the Ge

sub-cell, the slopes are larger and the  $\sigma_{\text{slope}}$  are a smaller fraction of the slope. This supports the opposite conclusion, that there is some, though weak, dependence of  $V_{\text{MAX}}$  on  $I_{\text{SC}}$ . The linear extrapolation will be applied to  $V_{\text{MAX}}$  even though it was not used for  $V_{\text{OC}}$ .

In table 5,  $\sigma_{\text{VMAX}}$  indicates the standard

deviation of the  $V_{\text{MAX}}$  measurements, while  $\sigma_{\text{line}}$  indicated the standard deviation from the line-of-best-fit.  $\sigma_{\text{line}}$  is useful for estimating calculation uncertainties.

For all four cells  $I_{\text{MAX}}$  is increasing and is nearly linear with  $I_{\text{SC}}$ . The extrapolation to  $I_{\text{SC}}$  (AM0) is a short extrapolation, a few percent. So the assumption that the relation stays linear is warranted.  $V_{\text{MAX}}$  vs  $I_{\text{SC}}$  shows some relationship, slightly decreasing with  $I_{\text{SC}}$ . The triple junction and top cell slopes for  $V_{\text{MAX}}$  are much larger than the uncertainty so these cells indicate at least some relationship between the two.

**Table 4. Linear Fit coefficients for  $I_{\text{MAX}}(I_{\text{SC}})$ .**

Type	Slope mA/mA	$\sigma_{\text{slope}}$	$\langle I_{\text{SC}} \rangle$ (mA)	$\sigma_{I_{\text{SC}}}$	$\langle I_{\text{MAX}} \rangle$ (mA)	$\sigma_{I_{\text{MAX}}}$	y-int (mA)
GaInP (Top)	0.953	0.007	64.47	0.01	61.76	0.05	0.3
GaAs (Mid)	0.877	0.126	68.91	0.01	63.94	0.04	3.5
Ge (Bottom)	0.832	0.075	132.46	0.01	113.64	0.43	3.4
TJ	0.905	0.005	63.18	0.01	61.19	0.03	4.1

**Table 5. Average  $V_{\text{MAX}}$  and slope of a linear fit**

Type	$\langle V_{\text{MAX}} \rangle$ V	$\sigma_{\text{VMAX}}$	$\sigma_{\text{line}}$	Slope V/mA	$\sigma_{\text{Slope}}$
GaInP (Top)	-1.258	0.004	0.003	0.0022	0.0004
GaAs (Mid)	-0.836	0.002	0.002	0.0014	0.0007
Ge (Bottom)	-0.189	0.002	0.002	-0.0003	0.0004
TJ	-2.351	0.009	0.007	0.0057	0.0008

## 4 Discussion

### 4.1 Flight

The results of compiling the flight data together are remarkably consistent with observations from the simple cell response model, equation 3.  $V_{\text{OC}}$  is only weakly dependent on  $I_{\text{SC}}$ , if not independent. The appearance of a dependence is attributed to temperature variations during the flight.  $I_{\text{MAX}}$  appears to be linear with  $I_{\text{SC}}$  as expected.  $V_{\text{MAX}}$  appears to have some weak dependence on  $I_{\text{SC}}$ . For the lower band gap cells it is within the scatter of the measurements, i.e. dominated by temperature effects. For higher band gap cells there appears to be some dependence but it is weak.

**Table 6. Estimated uncertainty in  $I_{\text{MAX}}$ .**

Type	I <sub>max</sub> (AM0)	$\sigma_{\text{Imax}}$ (AM0)	$\sigma_{\text{Rel}}$ (%)
InGaP (Top)	66.95	0.25	0.37
GaAs (Mid)	65.13	0.15	0.24
Ge Bottom	113.17	0.53	0.46
Triple	66.03	0.27	0.4

### 4.2 Results

#### 4.2.1 Uncertainties

Recent revisions in the procedure to account for ozone adsorption in the stratosphere has improved the reproducibility of  $I_{\text{SC}}$  measurements for the high altitude aircraft method. The uncertainty in flight-to-flight measurements is believed to be on the order of  $\pm 0.5\%$  (8).

The uncertainty in the extrapolation of a linear equation is obtained from

$$y \pm \sigma_y = y_0 \pm \sigma_{y_0} + (m \pm \sigma_m) * (x - x_0 \pm \sigma_x)$$

**Table 7. Estimated uncertainty in  $V_{\text{MAX}}$ .**

Type	V <sub>max</sub> (AM0)	$\sigma_{\text{Vmax}}$ (AM0)	$\sigma_{\text{Rel}}$ (%)
InGaP (Top)	-1.25	0.0040	-0.32
GaAs (Mid)	-0.83	0.0024	-0.28
Ge Bottom	-0.19	0.0023	-1.2
Triple	-2.32	0.0073	-0.32

$$\text{so, } \sigma_y^2 \sim \sigma_{y_0}^2 + (\Delta x \sigma_m)^2 + (m \sigma_x)^2$$

$\sigma_{y_0}$  is related to the scatter of the data around the line-of-best-fit.  $x_0$  is related to the position of the line and can be considered to be the average of the x-data,  $\langle x \rangle$ , and  $y_0$  can be considered to be  $\langle y \rangle$ .  $\sigma_x$  is the uncertainty in the  $I_{\text{SC}}$  measurement, about  $0.005 * I_{\text{SC}}$ , but obtained from the scatter in the flight  $I_{\text{SC}}$ (AM0) data.

### 4.3 Flight - Simulator Comparison

The extrapolation method is rather straight forward, and there is some theoretical basis to support its application. But an empirical comparison with the AM0 spectrum would additionally support application of the method. Ideally, the comparison should be with a high altitude balloon I(V) measurement. This had not yet been performed. However, NASA GRC has a triple source solar simulator (10), and when adjusted for the three sub-cells provides an initial comparison to the AM0 spectrum.

The NASA GRC X25 based multi-source solar simulator was used to produce I(V) curves for AM0. The simulator is adjusted to AM0 by adjusting the intensity of the three sources until each sub-cell produces the correct AM0 short circuit current. The figure 3 shows the resulting IV curves. Figure 3 also includes the X25 only I(V) curve for the triple junction cell. The difference in  $P_{MAX}$  noticeable.

In addition, I(V) curves using only the X25 source were taken for the purpose of comparing results with both the multi-source measurements and the flight measurement. The expectation is that the sub-cell measurements will agree closely for the three types of measurements. However, the difference between the triple junction results give indication of how the spectrum effects the measurements. The difference in the X25 and multi-source measurement gives a range with which to judge the agreement with the flight.

**Figure 3.** Laboratory I(V) measurements using the GRC Multi-source simulator. An X25 I(V) curve of the triple junction cell is included for comparison.

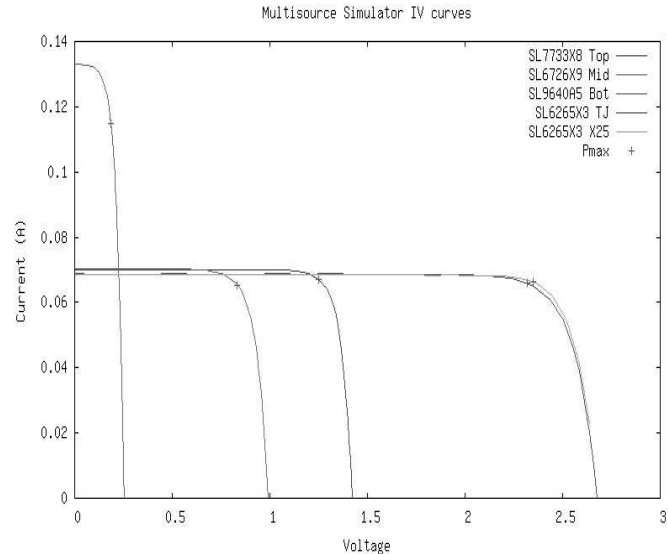


**Table 8.** Comparison of Flight IV characteristics with Multi-source Simulator and X25 (Xenon) Simulator at AM0.

#### High Altitude Aircraft

Cell	Type	Isc (mA)	Voc (V)	Imax (mA)	Vmax (V)	Pmax(mW)
SL7733X8	Top GaInP	69.91	1.4224	66.94	1.2462	83.42
SL6726X9	Mid GaAs	70.27	0.9934	65.13	0.8345	54.35
SL9640A5	Bot Ge	131.89	0.2574	113.77	0.1893	21.54
SL6265X3	Triple	68.52	2.6841	66.01	2.3221	153.28

#### Multisource

SL7733X8	Top GaInP	70.01	1.4174	67.15	1.2515	84.04
SL6726X9	Mid GaAs	70.28	0.9863	65.37	0.8336	54.49
SL9640A5	Bot Ge	132.89	0.2532	114.93	0.1848	21.24
SL6265X3	Triple	68.61	2.6583	65.96	2.3200	153.03

#### X25

SL7733X8	Top GaInP	69.99	1.3989	66.7	1.2512	83.46
SL6726X9	Mid GaAs	70.39	0.9807	64.98	0.8380	54.45
SL9640A5	Bot Ge	133.6	0.2537	113.02	0.1874	21.18
SL6265X3	Triple	68.62	2.6393	66.38	2.3493	155.95

### 4.3.1 Sub-Cells

The agreement in  $V_{OC}$  for the sub-cells is at the 1% level.  $I_{MAX}$  disagreement is near 0.7% for the top and middle cells while the bottom cell deviations are near 1.7%. The flight cell  $I_{MAX}$  values are between the X25 and Multi-source measurements. For  $V_{MAX}$  the deviations are near 0.5%, for the top and middle cells, but near 2.5% for the bottom cell.

### 4.3.2 Triple-Junction

The differences between the multi-source simulator and the X25 are given in table 9.

The principle difference in the Maximum power point for the X25 and multi-source simulator is due to  $V_{MAX}$ , at over 1% difference. The maximum power point difference with the flight data is near 0.1%. This is low enough to be considered fortuitous rather than an indication of the accuracy of the method, since it is much better than can be expected. However, it does indicate the method may be useful.

**Table 9.** Comparison of multi-source simulator measurements to X25 and flight derived results for the Triple Junction Cell.

Parameter	Multi-source / X25	Multi-source / Flight
$V_{OC}$	0.71%	0.97%
$I_{MAX}$	0.64%	0.08%
$V_{MAX}$	1.26%	0.09%

## 5 Conclusions

The most important result of this work is that the extrapolated maximum power point from flight data has excellent agreement with laboratory measurements from a triple source simulator. For the triple junction cell the agreement of both  $I_{MAX}$  and  $V_{MAX}$  was better than 0.1%. This agreement is much better than the accuracy of either the flight data, or the laboratory measurements, and should be regarded as fortuitous. However the agreement is certainly within the accuracy of the methods suggesting the method is sound.

The accuracy of the maximum power point measurements has been improved by using a quadratic fit to the points nearest the  $P_{MAX}$ . This has resulted in substantial reproducibility in  $P_{MAX}$  between different IV data sets.

In addition about 50 flight IV curves were used in the analysis improves the confidence in the result. The flight-to-flight reproducibility of the IV curve is excellent as illustrated by the small scatter of the data, especially of the  $I_{MAX}$  plots.

However this is only an initial examination of the method, performed with a single triple junction cell. The method should be verified by examining additional multi-junction cell and sub-cell sets. Also a comparison of this method with balloon flight data would improve confidence in the method. While balloon IV data may not be corrected to AM0,  $R_{SE} = 1$  AU, These method should be able to reproduce balloon flight data by extrapolating to the appropriate  $I_{SC}$ .

The power of this method becomes particularly important in the measurement of higher order multi-junction solar cells, such as four or five junction cells. The ground simulator adjustments for these cells may become prohibitive or, at best, difficult. This flight measurement method may provide a check and verification of the measurements and adjustment procedures.

## 6 References

- 1) D. Brinker, B. Anspaugh, R. Mueller, T. Gomez, E. F. Lisbona, K. Aoyama, M. Imaizumi, V. Pichetto, Y. Yiqiang, C. Goodbody, P. P. Jenkins, "Results From the 1<sup>st</sup> International AM0 Calibration Round Robin of Silicon and GaAs Solar Cells", Proceedings of 3<sup>rd</sup> World Conference on Photovoltaic Energy Conversion, Volume C, Osaka, Japan, 11-18 May 2003.
- 2) J.R. Woodyard and D.B. Snyder, "High Altitude Air Mass Zero Calibration of Solar Cells", 18<sup>th</sup> Space Photovoltaic Research and Technology Conference, Cleveland, Ohio, Sept. 16-18, 2003, NASA/CP-2005-213431, pp 148-165, 2005.
- 3) Philip Jenkins, David Brinker, and David Scheiman, "Uncertainty analysis of high altitude aircraft air mass zero solar cell calibration", V26-206, 26<sup>th</sup> PVSC; Sept 30-Oct.3, 1997; Anaheim, CA, IEEE 0-7803-3767-0/97.
- 4) P. Jenkins, TBP, 4<sup>th</sup> World Conference on Photovoltaic Energy Conversion 2006.



- 5) Henry W. Brandhorst Jr. and Earl O. Boyer, "Calibration of solar cells using high altitude aircraft", NASA Technical Note D-2508, February, 1965.
- 6) Scheiman, D.; Jenkins, P.; Brinker, D.; Snyder, D.; Baraona, C.; Rieke, W.; Blankenship, K.; and Tom, E., "A Summary of the 2000–2001 NASA GRC Lear Jet AM0 Solar Cell Calibration Program," SPRAT XVII, Cleveland, Ohio, September 2001.
- 7) D.B. Snyder, D.A. Scheiman, P.P. Jenkins, W.J. Rieke and K.S. Blankenship, "Ozone Correction for AM0 Calibrated Solar Cells for the Aircraft Method," 29th IEEE PVSC, paper 302.5, New Orleans, May 20-24, 2002.
- 8) D.B. Snyder, P. Jenkins, and D.A. Scheiman, "Historical Precision of an Ozone Correction Procedure for AM0 Solar Cell Calibration", 18<sup>th</sup> Space Photovoltaic Research and Technology Conference, Cleveland, Ohio, Sept. 16-18, 2003, NASA/CP-2005-213431, pp 166-169, 2005.
- 9) W.H. Press et al., *Numerical Recipes in C: The art of Scientific Computing*, Cambridge University Press, 2<sup>nd</sup> Edition, p108, 1992.
- 10) P. Jenkins, David Scheiman, David Snyder, "Design and Performance of a triple source Air Mass Zero Solar Simulator", 18<sup>th</sup> Space Photovoltaic Research and Technology Conference, Cleveland, Ohio, Sept. 16-18, 2003, NASA/CP-2005-213431, pp 134-138, 2005.